Effects of Wave–Wave and Wave–Mean Flow Interactions on the Growth and Maintenance of Transient Planetary Waves in the Presence of a Mean Thermal Restoring Force

Y. HAYASHI AND D. G. GOLDER

Geophysical Fluid Dynamics Laboratory/NOAA, Princeton University, Princeton NJ 08542

(Manuscript received 2 March 1987, in final form 1 June 1987)

ABSTRACT

In order to clarify the effects of wave–wave and wave–mean flow interactions on the growth and maintenance of extratropical tropospheric transient waves in the presence of a mean thermal restoring force, numerical experiments are conducted with the use of a dry general circulation model having a zonally uniform ocean surface. After the model has reached its steady state in the absence or presence of eddies, waves are allowed to grow from small disturbances by including all or some of the zonal wavenumber components.

In the presence of all the wavenumbers (1–21), ultralong waves (wavenumber 1–3) and cyclone-scale waves (wavenumber 4–9) initially grow as fast as short-scale waves (wavenumber 10–21), whereas ultralong waves do not initially grow as fast in the absence of wave–wave interactions. However, in the mature stage, ultralong waves attain a smaller amplitude in the presence of higher wavenumber components than they do in the absence of these components. This smaller amplitude is due to the fact that the mean baroclinicity is reduced by ultralong waves together with the higher wavenumber components to maintain equilibrium.

It is found that wave–wave interactions energetically play a more important role in the growth of ultralong waves than in their maintenance, being consistent with their nonlinear growth. This implies that the wave–wave energy transfer is sensitive to phase relations and is more efficient in the growing stage. It is also found that the ratio between the kinetic and available potential energies of ultralong waves is increased in the presence of wave–wave interactions. This implies that ultralong waves become more barotropic due to the nonlinear growth of external Rossby waves.

1. Introduction

In previous papers (Hayashi and Golder, 1977; 1983a,b; 1985) a spectral analysis was made of extratropical disturbances simulated by GFDL general circulation models. It was shown (Hayashi and Golder, 1983a) that westward moving ultralong waves were somewhat enhanced, while eastward ultralong waves were somewhat reduced by the effect of mountains. It was also found (Hayashi and Golder, 1983b) that westward moving ultralong waves were primarily maintained through the wave–wave transfer of available potential energy, while eastward moving ultralong waves were primarily maintained through the wave–mean transfer of available potential energy. The westward moving ultralong waves were associated with little vertical tilt, corresponding to external (equivalent barotropic) Rossby waves, while the eastward moving ultralong waves were associated with some vertical tilt, corresponding to baroclinic ultralong waves.

The growth of baroclinic ultralong waves may, to some extent, be due to the baroclinic instability of realistic zonal mean states. According to Hartmann (1979), eastward moving planetary waves having a narrow meridional width are associated with greater baroclinic instability than those having a wide meridional width such as those studied by Green (1960). Baroclinic ultralong waves may also be excited by wave–wave interactions. Nonlinear interactions between unstable and neutral baroclinic waves have been studied by Loesch (1974), Loesch and Domaracki (1977), Loesch and Peng (1978), Mansbridge and Smith (1983) and Nathan and Loesch (1984), (see also Haidvogel and Held, 1980; Salmon, 1980; Vallis, 1983).

Gall et al. (1979), MacVean (1985), Young and Villere (1985), and Young (1986) demonstrated with the use of simplified general circulation models that ultralong waves grew much more rapidly in the presence of cyclone-scale waves than expected from their linear growth rates. However, these simplified models are not appropriate for demonstrating how transient waves growing from small disturbances are maintained in their mature stage, since the zonal baroclinicity is eventually destroyed by the waves in the absence of a mean thermal forcing to restore the mean temperature gradient.

The present paper is intended to clarify the effects of wave–wave and wave–mean flow interactions on the growth and maintenance of transient planetary waves in the presence of a mean thermal restoring force:

1) To reexamine whether transient ultralong waves initially grow more rapidly in the presence of wave–

wave interactions than they do in the absence of the higher wavenumber components.

2) To examine whether transient ultralong waves attain a larger amplitude in their mature stage in the presence of higher wavenumber components than they do in the absence of these components.

3) To examine whether wave–wave energy transfer plays an important role not only in the growth of transient ultralong waves but also in their maintenance.

4) To examine whether transient ultralong waves become more barotropic due to the nonlinear growth of external Rossby waves.

For these purposes, numerical experiments have been conducted with the use of a dry general circulation model having a mean thermal restoring force. In section 2, the model used is described in more detail, while the results of the experiments are presented in sections 3 and 4. Conclusions and remarks follow in section 5.

2. Brief description of the model

The numerical experiments conducted for the present study used a hemispheric model (Northern Hemisphere) based on a 9-level, 21-wavenumber (rhomboidal truncation) spectral general circulation model, described in Manabe et al. (1979) and Gordon and Stern (1982). The biharmonic viscosity coefficient used in the present model is 0.25×10^{24} cm^4 s^{-1}. In order to eliminate the inherent nonlinearity in the condensation processes, moist convective adjustment was removed from the model. The dry convective adjustment was modified (see Smagorinsky et al., 1965) to adjust the lapse rate to a moist adiabat whenever the lapse rate became moist adiabatically unstable, since the dry adiabat is too unrealistic. For the effects of condensational heating on extratropical transient waves, the reader is referred to a numerical experiment of Hayashi and Golder (1981). In order to eliminate stationary waves, the original model's surface is replaced by an all ocean surface which has zonally uniform temperatures (see Fig. 2 of Hayashi and Golder, 1981). These temperatures were taken from the January zonal mean of ocean and ground temperatures of a 30-wavenumber spectral model without mountains. The insolation was fixed at the January mean value. The surface sensible heat fluxes were retained to restore the zonal mean temperature gradient, while the previous GCM experiments of Gall et al. (1979), MacVean (1985) and Young and Villere (1985) did not retain these fluxes nor introduce an alternative mean thermal restoring force.

In section 3, the initial zonal mean conditions for Experiment 1 (called day 0) were found by integrating the model, allowing only the zonally symmetric components (i.e., no eddies) until a steady state was reached. Small random perturbations with equal wavenumber amplitudes were then added to the temperature fields on day 0. The model was then repeatedly time integrated, allowing single, restricted or all the wavenumber components to interact.

In section 4, the time integrations for Experiment 2 were similar to those in Experiment 1 with the exception that the initial zonal mean state was taken from day 90 of Experiment 1 with all the wavenumbers.

3. Experiment 1

Figure 1a shows the latitude-height distribution of the mean zonal wind on day 0 in the absence of waves, while Fig. 1b is on day 90 when the zonal mean state has reached its steady state in the presence of fully grown transient waves of all the wavenumber components. It can be seen that transient waves somewhat reduce the intensity of the tropospheric jet and shift its position poleward from 25° to 45°N. The effect of planetary waves on the steady state zonal flow has been theoretically studied by Hayashi (1985a,b). The unrealistically strong stratospheric jet in both Figs. 1a and 1b is probably due to the absence of stationary waves, the perpetual January mean condition and the coarse vertical resolution.

a. *The growth of waves*

Figure 2a shows the time distribution of the tropospheric kinetic energy (205–1000 mb, Northern Hemi-

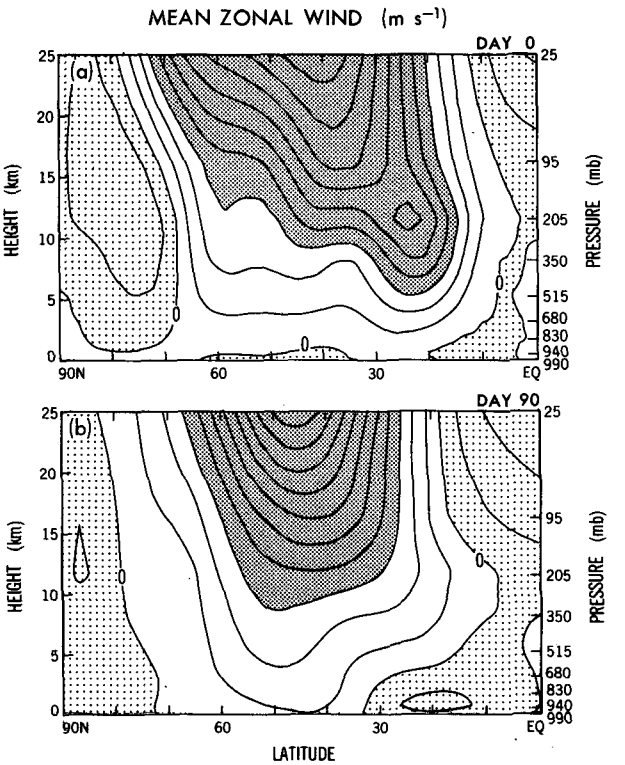

FIG. 1. Latitude–height distribution of the model's mean zonal wind on day 0 in the absence of waves (a) and day 90 in the presence of fully grown transient waves (b). Contour intervals 10 m s^{-1}. Dark shade > 30 m s^{-1}, light shade < 0.

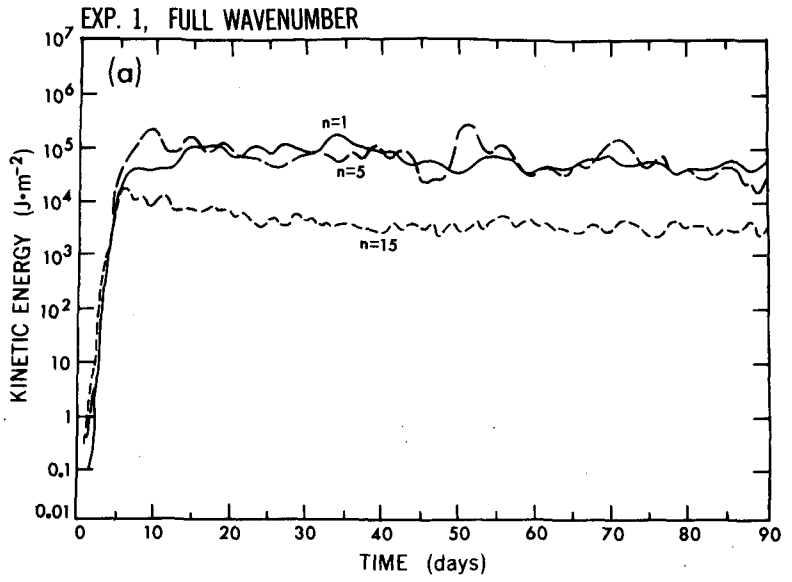
EXP. 1, FULL WAVENUMBER
(a)
n=1
n=5
n=15
KINETIC ENERGY (J•m⁻²)
TIME (days)

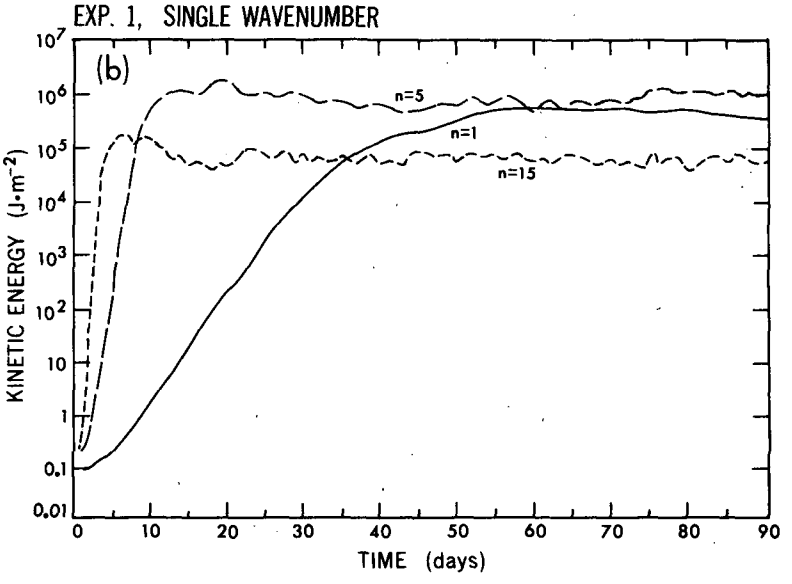
EXP. 1, SINGLE WAVENUMBER
(b)
n=5
n=1
n=15
KINETIC ENERGY (J•m⁻²)
TIME (days)

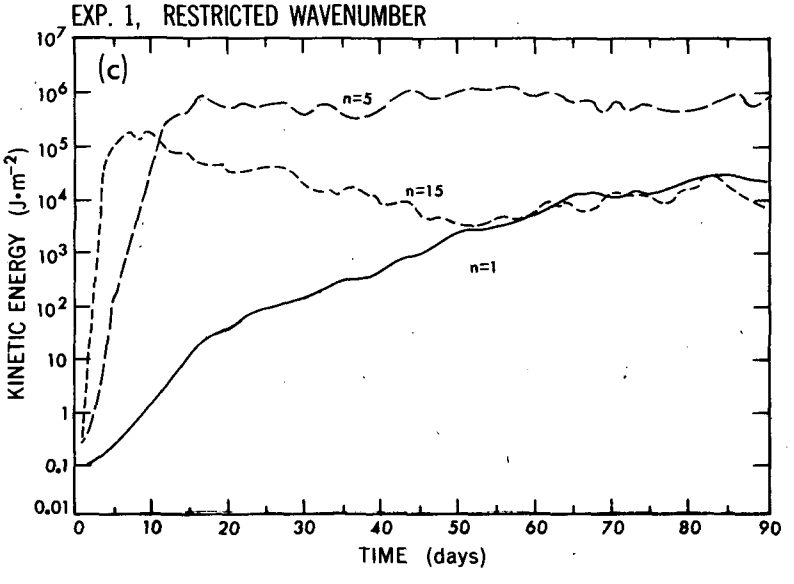
EXP. 1, RESTRICTED WAVENUMBER
(c)
n=5
n=15
n=1
KINETIC ENERGY (J•m⁻²)
TIME (days)

sphere) of wavenumber 1, 5 and 15 components of the model which allows all the wavenumber components (full wavenumber experiment). The stratospheric eddy kinetic energy was excluded from the vertical integral, since the stratospheric mean wind is unrealistically too strong. The hemispheric integral is essentially due to extratropical disturbances, since tropical disturbances do not attain a large kinetic energy in the absence of condensational heating. It is seen that the wavenumber 1 and 5 components initially grow as fast as the wavenumber 15 component but attain a larger amplitude in the mature stage than the wavenumber 15 component.

Figure 2b is the same as Fig. 2a except that a single wavenumber is allowed to grow without any wave–wave interactions (single wavenumber experiment). In contrast to the full wavenumber experiment, the wavenumber 1 component initially grows the slowest and the wavenumber 15 component grows the fastest. However, the wavenumber 15 component attains the smallest amplitude in the mature stage. This result is consistent with the growth of wavenumber 5 and 15 components in Gall's (1976) experiment in which a single wavenumber component was allowed to interact with the zonal mean, although his model did not have a mean thermal restoring force. In Gall's experiment, however, wavenumber 1 did not grow, since the initial zonal mean state of his dry model was taken from the time mean of a moist general circulation model which was associated with small baroclinicity.

In Gall's (1976) GCM experiment, only a single wavenumber was allowed to grow, while multiple wavenumbers were allowed simultaneously in the two level wave–mean flow interaction models of Pedlosky (1981), Hart (1981), and Klein and Pedlosky (1986). When only the wavenumber 1, 5 and 15 components are allowed to grow simultaneously in the present model (Fig. 2c), the wavenumber 1 component grows very slowly. This is due to the fact that the mean baroclinicity is reduced by the wavenumber 5 and 15 components. In this experiment, there are no wave–wave interactions among these three wavenumbers, since wavenumber 1 is not equal to the sum or difference of wavenumbers 5 and 15.

Figure 3a shows the time distribution of kinetic energy (205–1000 mb, Northern Hemisphere) of the wavenumber 1 component in the model which allows the full 21 wavenumber components (solid curve) and that which allows only a single wavenumber 1 component (dashed curve). Note that the wavenumber 1 component initially grows much more rapidly with wave–wave interactions (solid) than it does without these interactions (dashed). Interestingly, this component attains a smaller amplitude in its mature stage in the presence of higher wavenumbers (solid) than it does in their absence (dashed). This smaller amplitude is due to the fact that the mean baroclinicity is reduced by the wavenumber component together with the higher wavenumber components to maintain equilibrium. Figure 3b shows similar results for the wavenumber 3 component, although the effect of wave–wave interactions during the growing stage is less dramatic.

Figures 3c and 3d show the growth of the wavenumber 4–9 and 10–21 components, respectively, for the experiment allowing the full 21 wavenumber components (solid) and that allowing restricted 4–9 and 10–21 wavenumber components (dashed). Note that wave–wave interactions have little effect on the 4–9 and 10–21 components during their growing stage. Both these components attain somewhat smaller amplitudes in their mature stage in the presence of other wavenumbers (solid) than they do in the absence of the other components (dashed).

b. Eddy kinetic and potential energies

Table 1 shows the ratio (Kn/An) between kinetic (Kn) and available potential (An) energies of the wavenumber n components during the mature stage (day 31–90) of the experiments with full and restricted wavenumbers. It should be noted that wave–wave interactions increase this ratio for ultralong waves (wavenumber 1–3). This increase can be interpreted as the increase in the magnitude of external (equivalent barotropic) waves relative to that of baroclinic ultralong waves. In other words, wave–wave interactions make transient ultralong waves more barotropic. On the other hand, wave–wave interactions make short-scale transient waves (wavenumber 10–21) more baroclinic.

4. Experiment 2

In section 3, the initial (day 0) zonal mean condition was given by a zonal mean steady state in the absence of disturbances. In this section, these experiments have been repeated (Exp. 2) by replacing the initial mean states by those taken from day 90 of Exp. 1 in which all the wavenumbers were present.

FIG. 2. Time-distribution of the kinetic energy (205–1000 mb, Northern Hemisphere) of the wavenumber 1 (solid), 5 (dashed), and 15 (dotted) components of the model (Experiment 1) which allows (a) full wavenumber 1–21 components to grow. (b) As in (a) except that the model allows a single wavenumber component to grow. (c) As in (a) except that the model allows wavenumber 1, 5 and 15 components to grow simultaneously.

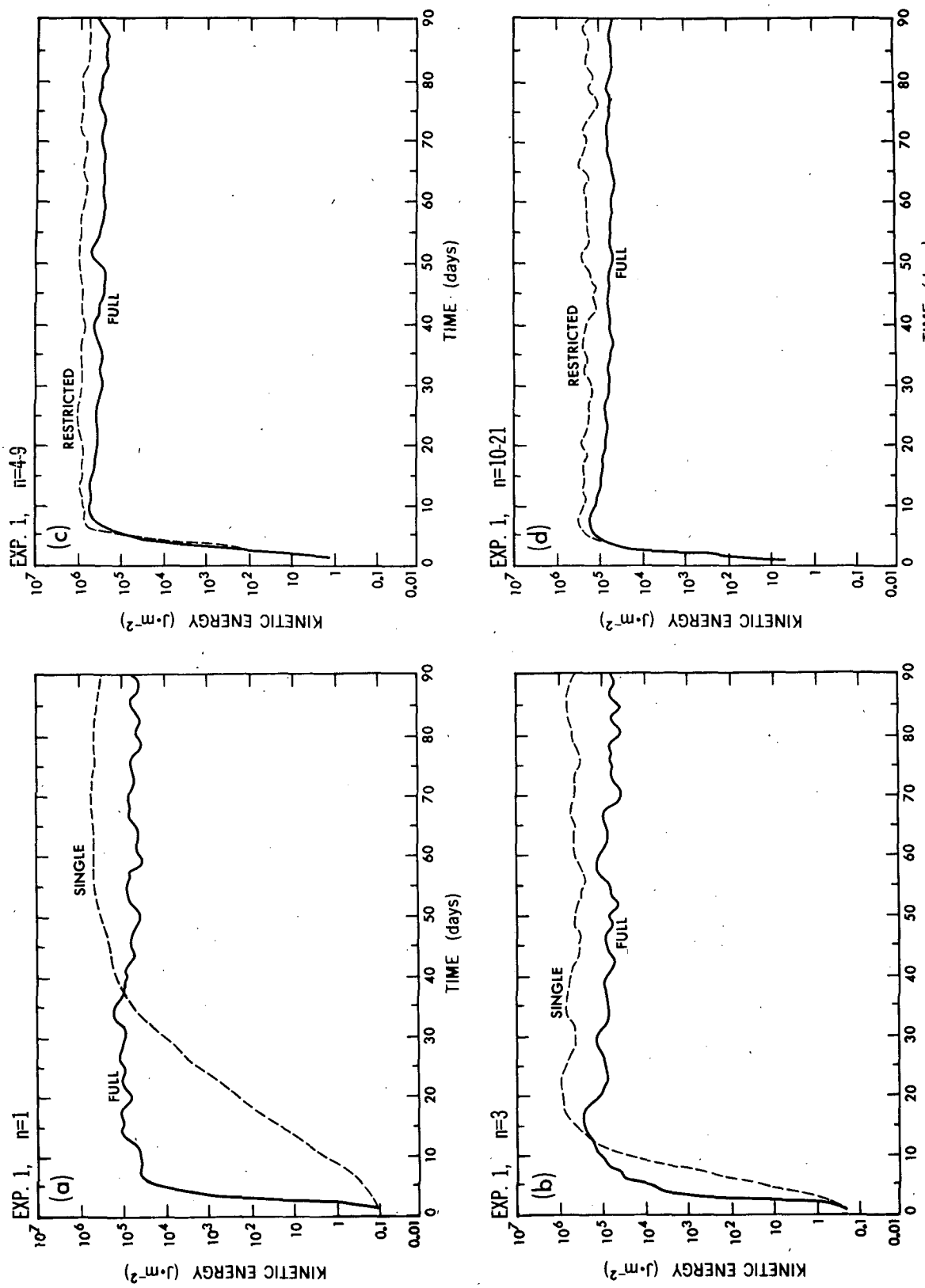

FIG. 3. Time distribution of the kinetic energy (205–1000 mb, Northern Hemisphere) of the wavenumber 1 component of the models (Experiment 1) which allow full wavenumber 1–21 components (solid) and (a) a single wavenumber 1 component (dashed). (b) As in (a) except for the wavenumber 3 component. (c) As in (a) except for the wavenumber 4–9 components. (d) As in (a) except for the wavenumber 10–21 components.

TABLE 1. Wavenumber distribution of the ratio (Kn/An) between kinetic (Kn) and potential (An) energies (Exp. 1, day 31–90, Northern Hemisphere, 205–1000 mb) of the models with full and restricted wavenumbers.

n	Full	Restricted
1	1.3	0.5
2	1.1	0.7
3	1.2	0.8
4–9	1.7	1.9
10–21	2.8	4.4

a. The growth of waves

Figure 4 is the same as Fig. 2 (Exp. 1) except that Exp. 2 has this new initial mean condition. In the presence of wave–wave interactions (Fig. 4a), the wavenumber 1 and 5 components grow nonlinearly after day 5 as fast as the wavenumber 15 component. In the absence of wave–wave interactions (Fig. 4b), the wavenumber 15 component grows the fastest and the wavenumber 1 component grows the slowest as in Exp. 1. However, these components grow more slowly in Exp. 2 than in Exp. 1. This is due to the fact that the new initial mean condition is associated with less baroclinicity. When wavenumbers 1, 5 and 15 are allowed to grow simultaneously (Fig. 4c), wavenumber 1 grows very slowly.

Figure 5 is the same as Fig. 3 (Exp. 1) except that Exp. 2 has the new initial mean condition. As in Exp. 1, the wavenumber 1 component (Fig. 5a) grows more rapidly in the presence of wave–wave interactions (solid curve) than it does in their absence (dashed curve). In the absence of other wavenumbers (dashed), this component grows more rapidly after day 20 than it does before day 10. This rapid growth rate is due to the fact that the mean baroclinicity becomes stronger with time due to the mean thermal restoring force (surface sensible heat flux) in the absence of other wavenumber components. When the zonal mean state is fixed in time and only the wavenumber 1 component is allowed to grow (dotted curve), it is seen that this component grows more slowly than when the zonal mean state is allowed to vary with time (dashed).

Figure 5b indicates that the wavenumber 3 component also attains a smaller amplitude in the presence of other wavenumbers (solid) than it does without these components (dashed). However, there is little difference during the growing stage between the single wavenumber experiments with and without the zonal mean fixed in time. This is because wavenumber 3 grows fast enough to offset the time change of the zonal mean state due to the mean restoring force. The dotted curve shows that, after 30 days, the kinetic energy of the wavenumber 3 component with the zonal mean fixed surpasses that without the zonal mean fixed. However, it is not meaningful to fix the zonal mean state in the mature stage when the amplitude is being saturated through wave–mean flow interactions.

Figures 5c and 5d indicate that the wavenumber 4–9 and 10–21 components also attain smaller amplitudes in the presence of other wavenumbers (solid) during the mature stage than they do in the absence of the other wavenumbers (dashed). There is hardly any difference in the growing stage between the restricted wavenumber experiments with (dotted) and without (dashed) the zonal mean state fixed in time. However, this result does not imply that wave–mean flow interactions do not affect these components, since the new initial zonal mean state has resulted from wave–mean flow interactions.

b. Energetics

These experiments with and without wave–wave interactions have demonstrated that wave–wave interactions play a more important role during the growing stage than in the mature stage. This suggests that wave–wave interactions energetically play a more important role in the growing stage than in the mature stage. In order to confirm this possibility, a comparison is made of the energetics of the waves during their growing and mature stages.

The wavenumber energy equation (Saltzman, 1957; Hayashi, 1980) is written as

$$\partial \mathrm{Kn}/\partial t + \partial \mathrm{An}/\partial t = \langle \mathrm{Km} \cdot \mathrm{Kn} \rangle + \langle \mathrm{Ko} \cdot \mathrm{Kn} \rangle + \langle \mathrm{Am} \cdot \mathrm{An} \rangle + \langle \mathrm{Ao} \cdot \mathrm{An} \rangle + \cdots. \quad (1)$$

Here, Kn and An are the kinetic and available potential energies for the zonal wavenumber n component. The $\langle \mathrm{Km} \cdot \mathrm{Kn} \rangle$ represents the "wave–wave transfer" of kinetic energy to the wavenumber n component by interaction among all the different (m) wavenumber components excluding 0 and n, while the $\langle \mathrm{Ko} \cdot \mathrm{Kn} \rangle$ represents the "zonal-wave transfer" of kinetic energy to the wavenumber n component by interaction between the zonal flow and the wavenumber n component. Similarly, the $\langle \mathrm{Am} \cdot \mathrm{An} \rangle$ and $\langle \mathrm{Ao} \cdot \mathrm{An} \rangle$ represent the "wave–wave and zonal-wave transfers" of available potential energy, respectively. The energy transfer spectra have been formulated from the equations of motion in the advection form. The explicit expressions can be found in the Appendix B of Hayashi and Golder (1983b).

Table 2a and Table 2b show the energy transfer terms for Exp. 2 in which all wavenumbers are allowed during the growing stage (day 5–15) and the mature stage (day 31–90), respectively. According to Table 2a, the wave–wave energy transfers $\langle \mathrm{Km} \cdot \mathrm{Kn} \rangle$ and $\langle \mathrm{Am} \cdot \mathrm{An} \rangle$ play a dominant role in the nonlinear growth of wavenumber 1, while these transfers are comparable to the zonal–wave transfer $\langle \mathrm{Ao} \cdot \mathrm{An} \rangle$ of available potential energy in the nonlinear growth of wavenumbers 2 and 3. There is also the possibility that $\langle \mathrm{Ao} \cdot \mathrm{An} \rangle$ itself has been increased by the wave–wave energy transfer $\langle \mathrm{Am} \cdot \mathrm{An} \rangle$ which enhances available potential energy. On the other hand, wavenumbers 4–9 and 10–21 lose their

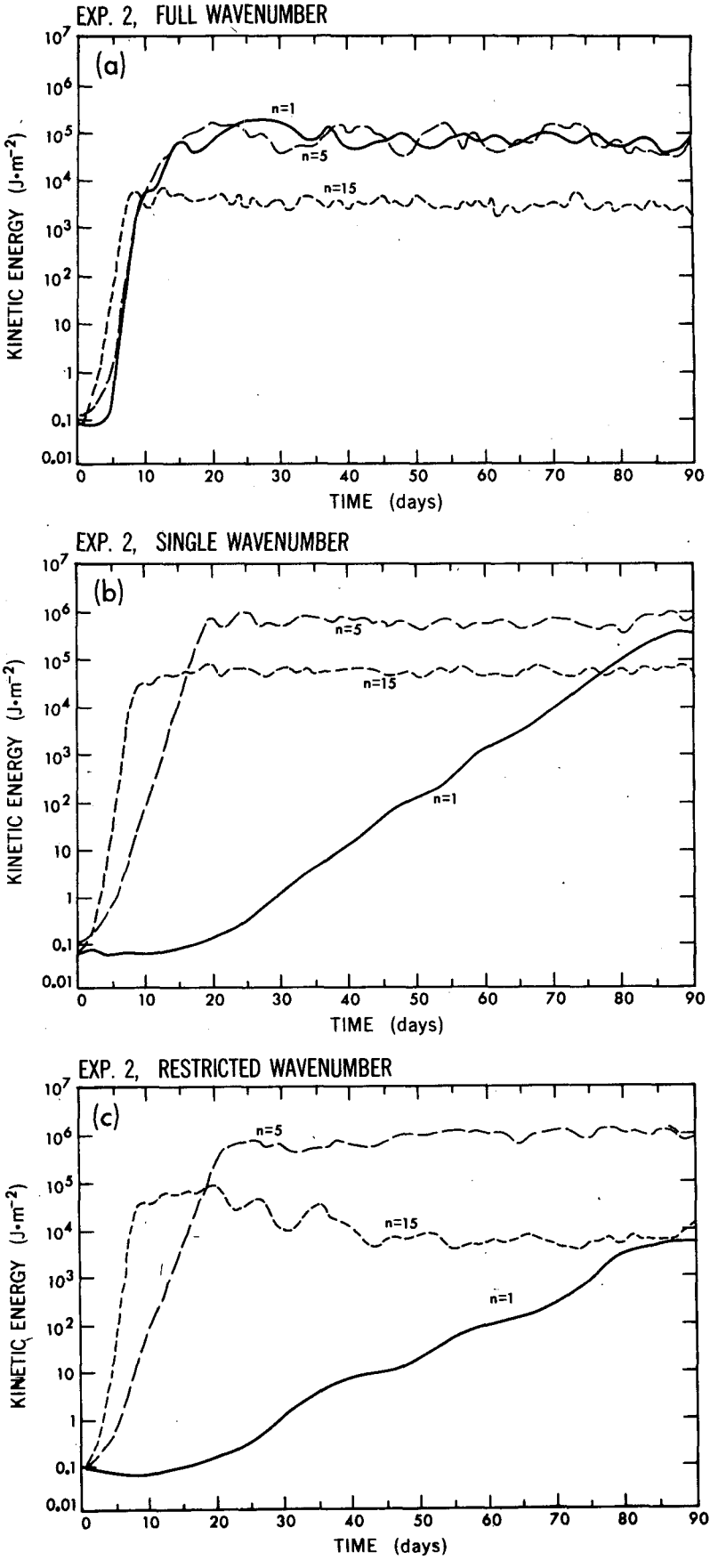

FIG. 4. As in Fig. 2 except for Exp. 2: (a) full wavenumbers, (b) a single wavenumber, (c) restricted wavenumbers.

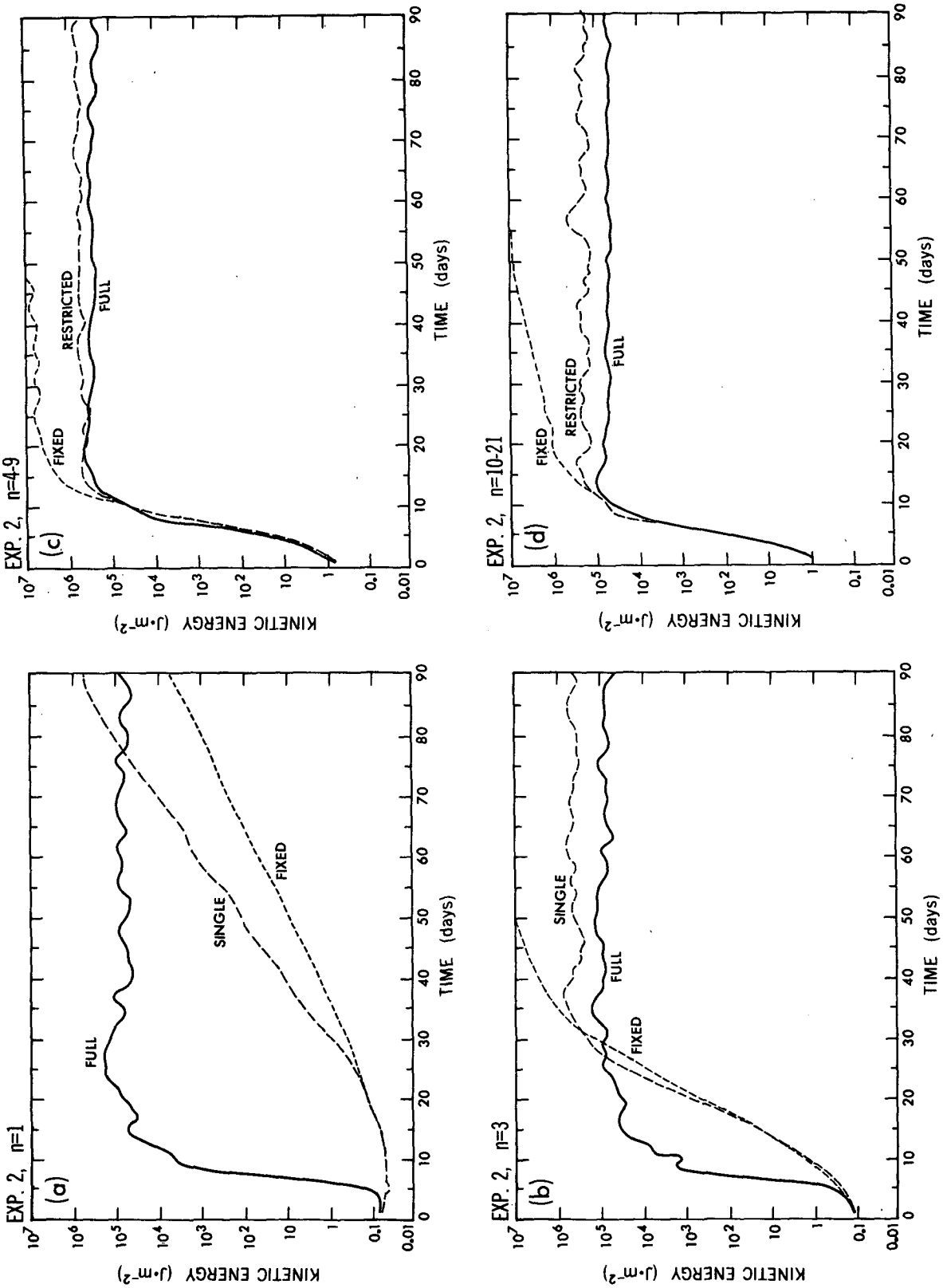

FIG. 5. As in Fig. 3 except for Exp. 2. Dotted curve indicates that the zonal mean is fixed in time: (a) wavenumber 1, (b) wavenumber 3, (c) wavenumbers 4–9, (d) wavenumbers 10–21.

energy to ultralong waves by wave–wave energy transfers $\langle Km \cdot Kn \rangle$ and $\langle Am \cdot An \rangle$. These losses are, however, negligible against their energy gain through the zonal-wave energy transfer $\langle Ao \cdot An \rangle$, being consistent with the result that wave–wave interactions had little effect on the amplitudes of the wavenumber 4–9 and 10–21 components during their growing stage.

In the mature stage (Table 2b), the wave–wave energy transfers $\langle Km \cdot Kn \rangle$ and $\langle Am \cdot An \rangle$ play a less important role in the maintenance of ultralong waves than they did in their growth. In particular, these transfers play a minor role for wavenumber 2 and 3 in spite of the larger amplitudes in the mature stage. This implies that wave–wave energy transfer is sensitive to phase relations and is less efficient when the amplitude is saturated. The wavenumber 10–21 components gain energy through the wave–wave energy transfers $\langle Am \cdot An \rangle$ and $\langle Km \cdot Kn \rangle$ occurring in the mature stage as observed (Saltzman, 1970), whereas these small-scale components lose energy to larger-scale waves by these energy transfers occurring in the growing stage. On the other hand, the wavenumber 4–9 components lose energy through the wave–wave energy transfers $\langle Km \cdot Kn \rangle$ and $\langle Am \cdot An \rangle$ in the mature stage as well as in the growing stage.

5. Conclusions and remarks

The present experiments have resulted in the following conclusions concerning the growth and maintenance of tropospheric extratropical transient waves.

1) Transient ultralong waves grow from small disturbances as fast as cyclone-scale and short-scale waves due to wave–wave interactions, whereas transient ultralong waves do not grow as fast in the absence of wave–wave interactions.

2) Transient ultralong waves attain smaller amplitudes during their mature stage in the presence of higher wavenumber components than they do in the absence of these components. This result is due to the fact that the mean baroclinicity is reduced by ultralong waves together with other waves to maintain equilibrium.

3) Wave–wave energy transfer plays a more important role in the growth of transient ultralong waves than in their maintenance, being consistent with their nonlinear growth. This implies that the wave–wave energy transfer is sensitive to the phase relations and is more efficient in the growing stage. Short-scale waves (wavenumber 10–21) lose energy to larger-scale waves through wave–wave energy transfer occurring during the growing stage, while they gain energy through this transfer during the mature stage.

4) Wave–wave interaction increases the ratio between the kinetic and available potential energy of transient ultralong waves. This implies that transient ultralong waves become more barotropic due to the nonlinear growth of external Rossby waves.

TABLE 2a. Wavenumber energy transfer spectra (10^{-3} W m^{-2}) averaged over day 5–15 (Exp. 2, Northern Hemisphere, 205–1000 mb).

n	1	2	3	4–9	10–21
$\langle Km \cdot Kn \rangle$	52	41	14	−87	−20
$\langle Ko \cdot Kn \rangle$	−9	−1	4	−117	−74
$\langle Am \cdot An \rangle$	65	46	52	−154	−11
$\langle Ao \cdot An \rangle$	37	58	78	1546	701

TABLE 2b. As in Table 2a except for day 31–90.

n	1	2	3	4–9	10–21
$\langle Km \cdot Kn \rangle$	40	25	4	−198	132
$\langle Ko \cdot Kn \rangle$	−10	−71	−184	−778	−16
$\langle Am \cdot An \rangle$	121	43	−9	−270	124
$\langle Ao \cdot An \rangle$	128	521	760	3202	234

Conclusion 1 demonstrates the importance of wave–wave interactions in the growth of ultralong waves from small disturbances. The fact that this conclusion does not crucially depend on the initial mean flow suggests that wave–wave interactions may also play an important role in the occasional amplification of observed ultralong waves. However, it is beyond the scope of the present experiments to explain this kind of amplification. It is of future interest to examine whether large scale initial errors grow rapidly in a forecast model in the absence of small scale initial errors.

Conclusion 2 suggests that cyclone-scale waves affect the amplitude of ultralong waves not only directly through wave–wave interactions but also indirectly through wave–mean flow interactions. The smaller amplitudes may be, to some extent, due to the fact that surface friction nonlinearly increases with the number of wave components.

Conclusion 3 suggests that the time mean energetics during the mature stage should not be interpreted as describing how waves grow energetically. This conclusion does not imply that wave–wave interactions play a less important role in the maintenance of ultralong waves than in their growth, since the zonal-wave transfer of energy may have increased as a result of wave–wave interactions.

Conclusion 4 is consistent with the result of Hayashi and Golder (1983b) that westward moving external ultralong waves are maintained primarily through the wave–wave energy transfer of available potential energy, while eastward moving baroclinic ultralong waves are maintained primarily through the zonal-wave transfer of available potential energy.

Acknowledgments. The authors are grateful to Dr. S. Manabe for his valuable advice and to Drs. I. M. Held and S. Feldstein for their appropriate comments on the original manuscript.

REFERENCES

Gall, R. L., 1976: Structure changes of growing baroclinic waves. *J. Atmos. Sci.*, **33**, 374–390.

——, R. Blakeslee and R. C. J. Sommerville, 1979: Cyclone-scale forcing of ultra-long waves. *J. Atmos. Sci.*, **36**, 1692–1698.

Gordon, C. T., and W. F. Stern, 1982: A description of the GFDL global spectral model. *Mon. Wea. Rev.*, **110**, 625–644.

Green, J. S. A., 1960: A problem in baroclinic stability. *Quart. J. Roy. Met. Soc.*, **86**, 237–251.

Haidvogel, D. B., and I. M. Held, 1980: Homogeneous quasi-geostrophic turbulence driven by a uniform temperature gradient. *J. Atmos. Sci.*, **33**, 2044–2660.

Hart, J. E., 1981: Wavenumber selection on nonlinear baroclinic instability. *J. Atmos. Sci.*, **38**, 400–408.

Hartmann, D. L., 1979: Baroclinic instability of realistic zonal mean states to planetary waves. *J. Atmos. Sci.*, **36**, 2336–2349.

Hayashi, Y., 1980: Estimation of nonlinear energy transfer spectra by the cross spectral method. *J. Atmos. Sci.*, **37**, 299–307.

——, 1985a: Theoretical interpretations of the Eliassen-Palm diagnostics of wave-mean flow interaction. Part I: Effects of the lower boundary. *J. Met. Soc. Japan*, **63**, 497–512.

——, 1985b: Theoretical interpretations of the Eliassen-Palm diagnostics of wave-mean flow interaction. Part II: Effects of mean damping. *J. Met. Soc. Japan*, **63**, 513–521.

——, and D. G. Golder, 1977: Space-time spectral analysis of mid-latitude disturbances appearing in a GFDL general circulation model. *J. Atmos. Sci.*, **34**, 237–262.

——, and ——, 1981: The effects of condensational heating on mid-latitude transient waves in their mature stage: Control experiments with a GFDL general circulation model. *J. Atmos. Sci.*, **38**, 2532–2539.

——, and ——, 1983a: Transient planetary waves simulated by GFDL spectral general circulation models. Part I: Effects of mountains. *J. Atmos. Sci.*, **40**, 941–950.

——, and ——, 1983b: Transient planetary waves simulated by GFDL spectral general circulation models. Part II: Effects of nonlinear energy transfer. *J. Atmos. Sci.*, **40**, 951–957.

——, and ——, 1985: Nonlinear energy transfer between stationary and transient waves simulated by a GFDL spectral general circulation model. *J. Atmos. Sci.*, **42**, 1340–1344.

Klein, P., and J. Pedlosky, 1986: A numerical study of baroclinic instability at large supercriticality. *J. Atmos. Sci.*, **43**, 1243–1262.

Loesch, A. Z., 1974: Resonant interactions between unstable and neutral baroclinic waves: Part I and Part II. *J. Atmos. Sci.*, **31**, 1177–1217.

——, and A. Domaracki, 1977: Dynamics of N resonantly interacting baroclinic waves. *J. Atmos. Sci.*, **34**, 22–35.

——, and M. Peng, 1978: On spectral energetics of resonantly interacting waves in the two-layer baroclinic model. *J. Atmos. Sci.*, **35**, 2373–2379.

MacVean, M. K., 1985: Long-wave growth by baroclinic processes. *J. Atmos. Sci.*, **42**, 1089–1101.

Manabe, S., and J. D. Mahlman, 1976: Simulation of seasonal and interhemispheric variations in the stratospheric circulation. *J. Atmos. Sci.*, **33**, 2185–2217.

——, D. G. Hahn and J. L. Holloway, Jr., 1979: Climate simulations with GFDL spectral models of the atmosphere: Effects of truncation. GARP Publ. Ser., No. 22, Vol. 1, 41–94.

Mansbridge, J. V., and R. K. Smith, 1983: On resonant interactions between unstable and neutral baroclinic waves. *J. Atmos. Sci.*, **40**, 378–395.

Nathan, T. R., and A. Z. Loesch, 1984: Resonant interactions between unstable and neutral baroclinic waves in a continuous model of the atmosphere. *Tellus*, **36A**, 320–335.

Pedlosky, J., 1981: The nonlinear dynamics of baroclinic wave ensembles. *J. Fluid Mech.*, **102**, 169–209.

Salmon, R. L., 1980: Baroclinic instability and geostrophic turbulence in a simple case. *Geophys. Astrophys. Fluid Dyn.*, **15**, 167–211.

Saltzman, B., 1957: Equations governing the energetics of the large scales of atmospheric turbulence in the domain of wavenumber. *J. Meteor.*, **14**, 513–523.

——, 1970: Large-scale atmospheric energetics in the wavenumber domain. *Rev. Geophys. Space Phys.*, **8**, 289–302.

Smagorinsky, J., S. Manabe and J. L. Holloway, Jr., 1965: Numerical results from a nine-level general circulation model of the atmosphere. *Mon. Wea. Rev.*, **93**, 727–768.

Vallis, G. K., 1983: On the predictability of quasi-geostrophic flow: The effects of beta and baroclinicity. *J. Atmos. Sci.*, **40**, 10–27.

Young, R. E., 1986: Effects of eddy initial conditions on nonlinear forcing of planetary scale waves by amplifying baroclinic eddies. *J. Atmos. Sci.*, **43**, 3241–3249.

——, and G. L. Villere, 1985: Nonlinear forcing of planetary scale waves by amplifying unstable baroclinic eddies generated in the troposphere. *J. Atmos. Sci.*, **42**, 1991–2006.